CHEMISTRY
A European Journal

A Journal of
ChemPubSoc Europe

Accepted Article

Title: Biocatalytic strategies towards [4+2] cycloadditions

Authors: Benjamin R. Lichman, Sarah E. O'Connor, and Hajo Kries

To be cited as: *Chem. Eur. J.* 10.1002/chem.201805412

Link to VoR: http://dx.doi.org/10.1002/chem.201805412

Supported by
ACES

WILEY-VCH

10.1002/chem.201805412
WILEY-VCH

MINIREVIEW

Biocatalytic strategies towards [4+2] cycloadditions

Benjamin R. Lichman,[b, c] Sarah E. O'Connor[b] and Hajo Kries*[a]

Abstract: Long sought after [4+2] cyclases have sprouted up in numerous biosynthetic pathways in recent years, raising hopes for biocatalytic solutions to cycloaddition catalysis, an important problem in chemical synthesis. In a few cases, detailed pictures of the inner workings of these catalysts have emerged, but intense efforts to gain deeper understanding are underway by means of crystallography and computational modelling. This review aims to shed light on the catalytic strategies that this highly diverse family of enzymes employs to accelerate and direct the course of [4+2] cycloadditions with reference to small molecule catalysts and designer enzymes. These catalytic strategies include oxidative or reductive triggers and lid-like movements of enzyme domains. A precise understanding of natural cycloaddition catalysts will be instrumental for customizing them for various synthetic applications.

1. Introduction

Biocatalysis and synthetic organic chemistry play by the same physico-chemical rules, but their strong suits are fundamentally different. A case in point are cycloaddition reactions: their wide use in synthetic organic chemistry contrasts with their scarcity in biological systems. When Diels and Alder first discovered synthetic [4+2] cycloadditions they proposed that these reactions may be responsible for the formation of natural products;[1] this prediction was accurate, but enzymes performing cycloadditions remained elusive for many decades.

Remarkably, Diels-Alderases raised from antibodies in the laboratory preceded isolation of natural enzymes by several years.[2] Although Diels-Alder reactions had been implicated in biosynthetic pathways since at least the 1970s,[3] it took until the mid-1990s for the first observation of natural enzymatic activity catalysing a Diels-Alder reaction.[4] In recent years, a "gold rush" for enzymatic cycloadditions has unveiled a number of these biosynthetic transformations. However, the natural reactions play a different role to those employed by synthetic chemists. While synthetic chemists often harness intermolecular cycloadditions as a retrosynthetic disconnection, the natural examples tend to happen intramolecularly and occur late in the biosynthetic pathway.

In this review, we will explore the catalytic mechanisms of natural and unnatural [4+2] cyclases and compare them to chemical strategies. Determining accurate mechanisms of enzyme catalysed cycloadditions has proved to be challenging. The atom connectivity of reactants and products can readily be used to qualify a reaction as a formal [4+2] cycloaddition, but considerable debate concerns the degree of synchronicity[5] which is often taken as a criterium for "true" Diels-Alder reactions. As intriguing and important as the mechanistic study of enzymatic cycloadditions is, knowing the synchronicity of bond formation events is not a priority for biocatalytic applications. Hence, we will cover enzymes catalysing formal [4+2] cycloadditions whether or not the detailed mechanism is known. This includes Diels-Alderases catalysing a concerted [4+2] cycloaddition and enzymes employing stepwise Michael-aldol mechanisms. We will consider [4+2] cyclases to be any enzyme catalysing a reaction in which reactants with four and two atoms are connected to form a cycle of six while undergoing a reduction in bond multiplicity.[6,7] Compared to the excellent reviews of the past years covering cyclases,[7–14] here we also highlight the newest discoveries in plants and focus particularly on the catalytic devices of the natural enzymes, designer enzymes and small molecule catalysts.

[a] Dr. H. Kries
Independent Junior Research Group
Biosynthetic Design of Natural Products
Leibniz Institute for Natural Product Research and Infection Biology
Hans Knöll Institute (HKI Jena)
Beutenbergstr. 11a, 07745 Jena, Germany
E-mail: hajo.kries@leibniz-hki.de
[b] Dr. B. R. Lichman, Prof. Dr. S. E. O'Connor
Department of Biological Chemistry
The John Innes Centre
Colney Lane, Norwich, UK
[c] Dr. B. R. Lichman, current address:
Department of Biology, University of York, York, YO10 5YW, UK

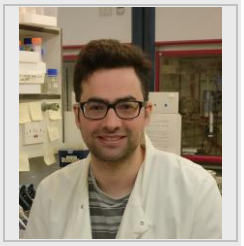

Benjamin Lichman obtained his Master's degree at the University of Cambridge followed by his PhD at University College London. After his PhD studies he joined Prof. Sarah O'Connor's group at John Innes Centre as a post-doctoral researcher, where he worked on the discovery and characterisation of iridoid forming enzymes. He is currently a Lecturer in Plant Biology at the University of York. His research focusses on the discovery, evolution and applications of enzymes from plant specialised metabolism

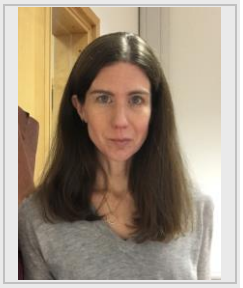

Sarah O'Connor received her degrees in chemistry from the University of Chicago (BS) and MIT (PhD), and performed her post-doctoral work at Harvard Medical School. She has been a Professor and Project Leader in Biological Chemistry at the John Innes Centre since 2011. Her research interests focus on the natural products of plants, with a particular interest in the iridoids and alkaloids. Her research group takes a broad approach to understanding plant biosynthetic pathways, ranging from gene discovery, mechanistic enzymology, and metabolic engineering.

10.1002/chem.201805412

Hajo Kries obtained his doctoral degree from ETH Zurich (Switzerland) for his work in the lab of Donald Hilvert on enzyme design and engineering. After postdoctoral studies in Sarah E. O'Connor's lab at the John Innes Centre (Norwich, UK), he became junior group leader at the Hans Knöll Institute in Jena, Germany. He is currently investigating engineering methods for nonribosomal peptide synthetases.

2. How chemists accelerate [4+2] cycloadditions

Although chemists have often turned to nature for inspiration, small-molecules catalysing cycloadditions were synthesised long before biocatalysts for these reactions were designed or discovered. Chemical catalysis of Diels-Alder reactions, for example with simple Lewis acids such as aluminum trichloride, can achieve rate accelerations of 10^5 fold; the same range as typical, moderately efficient enzyme catalysts.[15] This spectacular effect powers asymmetric catalysts that accelerate and direct the Diels-Alder reaction into a single stereochemical outcome.[16,17] The Lewis acid metal centre of these catalysts provides the core catalytic effect, whilst sterically demanding ligands close off undesired routes by favouring specific orientations of the reactants. Electronically, cycloaddition catalysis has been explained by a narrowing of the energy gap between the frontier orbitals of the diene and, through binding of the Lewis acid, the more electron-depleted dienophile.[5,18]

For biological cyclases to become relevant in industrial biocatalysis, they must be able to compete with enantioselective chemical catalysts. These chemical catalysts have been meticulously designed for high catalytic efficiency and enantioselectivity and thus provide a rigorous reference point for discussing their biological counterparts (Scheme 1). Corey's C2 symmetric aluminum diamine **1** is illustrative of the chemo-catalytic approach.[19] Here, the aluminum metal center is coordinated by the dienophile with the less hindered lone pair opposite the oxazolidinone moiety. Pi-pi interactions likely govern the preference of the vinyl residue to point towards the phenyl group of the catalyst and the cyclopentadiene attacks with *endo* preference from the less shielded face. As a result, the cycloaddition product **2**, an intermediate in the total synthesis of prostaglandin, is formed with 96% enantiomeric excess.

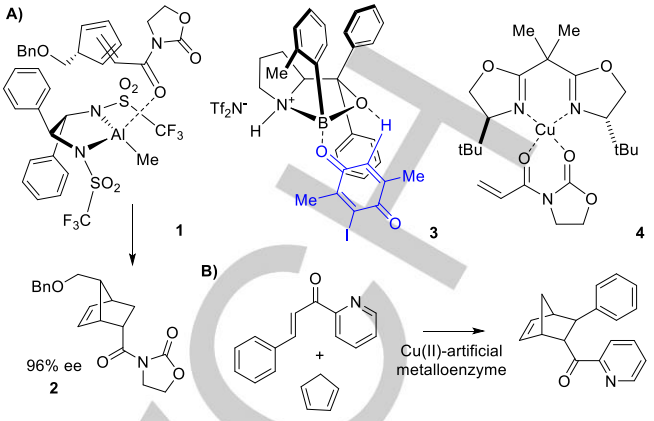

Scheme 1. A) Small molecules as enantioselective catalysts for Diels-Alder reactions.[16,19] **B**) A reaction catalysed by artificial metalloenzymes.

Conformational restriction of the dienophile is crucial for the success of enantioselective catalysts that use only monodentate coordination, such as the aluminum diamines. In Corey's oxazaborolidine ligand complex **3**, a weak interaction with the C-alpha hydrogen of the ketone ligand has been proposed to account for this restriction, furnishing excellent enantioselectivities up to 99% ee.[19] Evan's cationic copper(II) bisoxazolines are noteworthy because copper(II) complexes are relevant for the construction of artificial metalloenzymes.[20] Due to the bidentate coordination of the dienophile and the C2 symmetry at the distorted square planar copper centre in complex **4**, predictions of the transition state are straightforward, and it follows that facial selectivity of the dienophile is controlled by the bulky tert-butyl groups.[21]

For cycloadditions featuring hydrophobic reactants, for example the Diels-Alder reaction of methylvinylketone and cyclopentadiene, solvent selection can be influential. In a polar solvent like water, greasy reactants will associate with each other, and this hydrophobic proximity effect can accelerate the Diels-Alder reaction by two to three orders of magnitude.[22] To achieve rate accelerations, an enzyme in aqueous solution must therefore provide more than the hydrophobic effect in solvent alone. A more exotic catalytic device not directly available to enzymes are high pressures of several thousand atmospheres, which have been useful in mechanistic studies and total synthesis.[23,24] High pressures drive formation of the, relative to the reactants, more compact Diels-Alder transition state.[25]

Enantioselective catalysts often show high stereoselectivity like enzymes but compare poorly in terms of catalytic efficiency: reactions typically take days to reach completion. For copper bisoxazolinones, dissociation constants in the high millimolar range have been reported.[26] Given the open and solvent exposed arrangement of substrates on the metal centre of a small molecule chiral catalyst, weak binding and a generally large substrate scope are unsurprising. Currently, although cyclases are not able to supplant small molecule catalysts, with further optimisation they may provide stronger binding and higher catalytic efficiencies.

3. Metals for speed, protein for selectivity

Artificial metalloenzymes hold great promise as designer biocatalysts with bespoke binding pockets, superior selectivities to small molecule catalysts and, perhaps, additional catalytic groups for faster reaction rates.[20] Several exquisite examples have been created in the laboratory. Metallo-cyclases require the anchoring of the catalytic metal complex inside a proteinaceous pocket whilst also accommodating the substrates in the correct orientation for selective catalysis. For instance, Reetz and co-workers have bound a Cu(II)-phthalocyanine complex to bovine serum albumin (BSA), a protein with a universal tendency to accommodate hydrophobic molecules on its surface (Scheme 1B).[27] Upon protein addition, the high endo:exo selectivity of the catalyst (96:4) was maintained while the chiral protein environment conferred a 93% enantiomeric excess. The catalytic rate, however, dropped slightly compared to the free ligand. With 2 mol% catalyst loading of a 66 kDa protein, the protein exceeded the product mass by far, underlining the challenge to create designer biocatalysts with fast catalytic rates (i.e. k_{cat}) and high turnover numbers (TON).

With protein catalysts comes the promise of genetic fine tuning and metalloenzymes are no exception to this.[28,29] Enzyme binding pockets enclose substrates with a shell of protein side-chains that can be mutated to a vast variety of shapes and decorated with charges and H-bonding donors and acceptors. Bos and colleagues installed a conjugation site for bromoacetamide ligands by introducing the mutation Met89Cys into the small, homodimeric Lactococcal multidrug resistance Regulator (LmrR) protein (Scheme 1B).[30] By conjugating a phenanthroline ligand and adding copper, an enantioselective catalyst was created reaching a good enantiomeric excess of 97 % (endo:exo = 95:5). In this case, conjugation to LmrR not only rendered the reaction enantioselective but also accelerated it, as indicated by a 4.7-fold increase in yield after three days reaction time. The active site was responsive to mutation which could perhaps be exploited by more comprehensive mutational screens. Metallo-cyclases appear to provide the best of both worlds for catalyst design: catalysis is provided by the metal centre and selectivity by the protein. This separation of roles may ultimately make these systems easier to control and modify than natural cyclases, in which catalysis and selectivity are intimately coupled within the protein structure. The presence of a protein scaffold, amenable to mutation and directed evolution,[31] makes these synthetic enzymes a promising prospect for industrial biocatalysis. Despite the abundance of natural enzymes with catalytic metal centres, and the utility of metals in cycloaddition catalysis, natural [4+2] cyclases utilising metal catalysis have not been observed. Instead, enzymes using other catalytic strategies have been discovered.

4. Pulling the trigger

Biosynthesis is a system replete with reactive intermediates and cascade-like multiple transformations. This has led to different strategies for catalysing cycloadditions which take advantage of multiple, cascaded reaction steps. For example, enzymes have been discovered that couple cyclisation to redox steps, a reduction or oxidation step effectively 'pulling the trigger' by creating a reactive intermediate primed to undergo subsequent cyclisation.

4.1. Oxidation: solanapyrone synthase

Solanapyrone synthase (SPS) catalyses an NAD^+ dependent oxidation prior to [4+2] cyclisation (Scheme 2A). The crude enzyme was isolated from the fungal pathogen *Alternaria solani* and shown to catalyse the *exo*-selective formation of the decalin moiety found in the solanapyrones. In the absence of the cell-free extract, the aldehyde prosolanapyrone III (**6**) spontaneously cyclises to form a mixture of the *exo* and *endo* adducts **7** and **8** in a 3:97 ratio. In contrast, the crude enzyme selectivity was 87:13.[4] The crude enzyme was also shown to perform kinetic resolution of the cyclised (±)-solanapyrone B through enantioselective oxidation to (-)aldehyde solanapyrone A (**7**). This stereoselectivity indicates recognition of the decalin by the oxidase and perhaps coupling of the oxidation and cyclisation steps.

When the solanapyrone biosynthetic gene cluster was identified and cloned, Sol5, a flavin-dependent oxidase (SPS), was determined to be responsible for both the oxidation and cyclisation reactions.[32] The purified, bifunctional enzyme can convert the alcohol substrate prosolanapyrone II (**5**) to solanapyrone via a two-step oxidation-cyclisation reaction with high enantioselectivity (99% *ee*). Notably, the cycloaddition activity of the enzyme was observed to denature more rapidly than the oxidation activity, suggesting there may be a structural element specific to cyclisation.[33] Oxidation of the hydroxymethyl in prosolanapyrone II (**5**) lowers the LUMO of the dienophile, which promotes the cycloaddition. Further catalytic interactions with Sol5 to promote cyclisation have not yet been identified. To account for the perfect enantiomeric purity, the enzyme must control cyclisation, though the presence of 13 % endo-product **8** suggests imperfect enzyme selectivity.

4.2. Reduction: iridoid synthase

Reduction, too, can pave the way for a cyclisation reaction, as exemplified by iridoid synthase (ISY). Iridoid monoterpene biosynthesis in plants starts with the reductive cyclization of 8-oxogeranial **9** to nepetalactol (Scheme 2B). Through an accumulation of evidence, it has become apparent that the first enzyme in this process, ISY,[34–37] catalyses the stereoselective 1,4-reduction of 8-oxogeranial **9**, but not subsequent cyclisation. After forming the uncyclised and reactive enolate via reduction, ISY does not catalyse its cyclisation, but appears to release it as

10.1002/chem.201805412

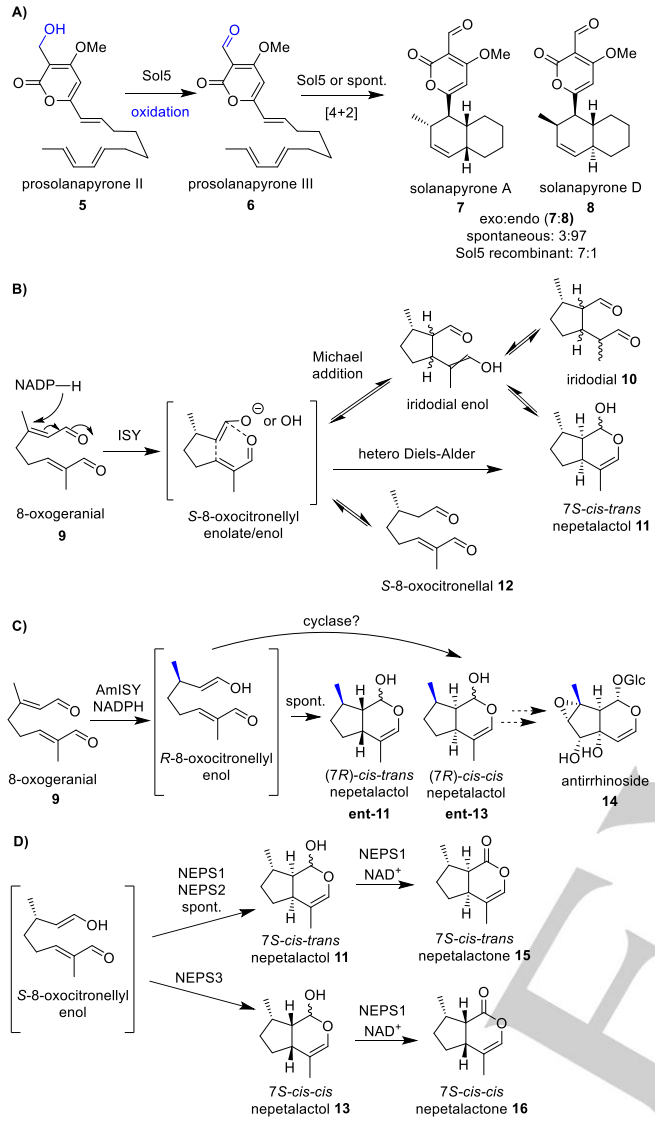

Scheme 2. A) Solanapyrone synthase (SPS) and **B-D**) iridoid synthase (ISY) trigger cyclizations by oxidation and reduction reactions, respectively.

a product. This intermediate then cyclises or unproductively tautomerises outside the ISY active site. Hence, in conversion assays with CrISY (*Catharanthus roseus*) and 8-oxogeranial **9**, small amounts of multiple reaction products are consistently observed, in addition to the expected bicyclic (7*S*)-*cis-trans*-nepetalactol **11**. These include monocyclic iridodials with varying bridge stereochemistry and the uncyclised 8-oxocitronellal **12**.[38] Strikingly, the proportion of diastereomeric products formed is independent of the ISY employed, even in the case of AmISY (*Antirrhinum majus*, snapdragon) which produces the 7*R* product series in contrast to the 7*S* series produced by CrISY (Scheme 2C).[38] Instead, the distribution of products is affected by conditions such as buffer type and concentration, with increased buffer concentrations resulting in greater proportions of side-products. These results indicated that the cyclisation occurs in the solvent, with the buffer acting as a general acid catalyst.[39]

The crystal structures of CrISY co-crystallised with cofactor and substrate or inhibitor support this: the substrate binds in a linear conformation conducive to reduction but not cyclisation.[40–42] Investigation into the cyclisation propensity of substrate analogues suggested nepetalactol formation occurs via step-wise Michael addition, and not Diels-Alder cyclisation (Scheme 2B);[43] it now appears these experiments were probing not the enzymatic but the general-acid/buffer catalysed mechanism. Although it has become clear that iridoid synthase does not control the cyclisation step, the abundance of certain nepetalactol isomers in some plants led to the hypothesis that stereocontrol may be provided by a second enzyme, which will be discussed in the next section.

5. Controlling (stereo)selectivity

Molecular complexity is generated at cycloaddition steps, and through controlling the chemo and stereoselectivity of these steps diverse products can be obtained. Hence, in some biosynthetic pathways, cycloaddition steps constitute crucial metabolic branch points. Interestingly, there are multiple examples where closely related enzymes appear to catalyse divergent selectivities.

5.1. Nepetalactol-related short-chain reductases

We have recently identified three enzymes from the catmint *Nepeta mussinii* which control formation of nepetalactol, precursor to the cat attractant nepetalactone.[36,39] These enzymes, the nepetalactol-related short-chain-dehydrogenase/reductases (NEPS), appear to be specific to the *Nepeta* genus and are putative [4+2] cyclases. The activities of these NAD-dependent enzymes are revealed in cascade reactions with 8-oxogeranial **9**, ISY and appropriate cofactors. NEPS1 seems to be a bifunctional cyclase and dehydrogenase, promoting formation of *cis-trans*-nepetalactol **11** at the expense of side products and oxidising it into nepetalactone (Scheme 2D). With NEPS2, only *cis-trans* cyclase activity was found. NEPS3 has the most interesting activity because it overrules the non-enzymatic cyclisation selectivity and promotes formation of *cis-cis*-nepetalactol **13**, an isomer formed in only trace amounts without enzyme. Despite the presence of the nicotinamide co-factor, none of the NEPS enzymes catalyse the ISY reaction, reduction of 8-oxogeranial **9**. Although they can accept 8-oxocitronellal **12** as a substrate, this occurs with poor yields and only in the presence of buffer. Altogether, the data indicate that NEPS1-3 accept 8-oxocitronellyl enol, the short-lived product of ISY, as a substrate and perform cyclisation in a redox-neutral manner.

Based on structural and mutational analysis of NEPS1 and NEPS3, it appears that whilst both enzymes provide selectivity in the [4+2] cyclisation, they do so via different mechanisms. NEPS1 catalysed *cis-trans* cyclisation appears robust to mutation, and the enzyme may merely be protecting the reactive intermediate from the solvent, preventing the formation of side products. NEPS3, on the other hand, must be actively binding its substrate

10.1002/chem.201805412

in a specific conformation to yield the *cis-cis* isomer. A similar, *cis-cis* selective enzyme might work together with AmISY in antirrhinoside biosynthesis (Scheme 2C). NEPS3 interactions with the reactive intermediate appear to be controlled by oxyanion interaction with Ser154, though further structural and computational data are required to fully understand this cyclase's mechanism.

5.2. Catharanthine and tabersonine synthase

The biosynthesis of the cancer drug vinblastine in the plant *Catharanthus roseus* provides a remarkable example in which a single precursor (dehydrosecodine [**15**]) is cyclized to two different products (catharanthine [**16**] and tabersonine [**17**]) by two chemo and stereoselective [4+2] cyclases (Scheme 3A). Decades of biomimetic chemical investigation[44–47] support the notion that divergent Diels-Alder cyclisations of the hypothetical intermediate dehydrosecodine (**15**) could provide the two distinct scaffolds, catharanthine (**16**) and tabersonine (**17**), via an inverse- and a normal electron-demand Diels-Alder reaction, respectively. Through a combination of *in planta* silencing, bioinformatics and recombinant assays, the enzymes controlling this crucial branch point have finally been identified.[48,49] Two closely related α/β-hydrolase enzymes with 78% sequence identity, catharanthine synthase (CS, HL1) and tabersonine synthase (TS, HL2), act as divergent, stereoselective cyclases. The role of CS and TS was indicated by gene silencing *in planta* and then verified by reconstitution of the pathway *in vitro* and *in planta*.

The enzymes CS and TS have been shown to control the stereoselectivity of a [4+2] cyclisation reaction, but their identity as 'dedicated' Diels-Alderases can only be confirmed when their substrate is known: to date, the cyclisation activity has only been observed as a part of the multi-enzyme cascade. The dehydrosecodine intermediate (**15**) remains the most likely candidate for the Diels-Alder step, but the divergent reactions would proceed via specific transition states. Selectivity may be achieved via steric effects, i.e. controlling the conformation of the substrate in the active site, or electronic effects, i.e. lowering the LUMO to reduce the transition state energy. The latter possibility is intriguing as the reactions have different electronic characteristics (inverse electron demand versus normal electron demand) so the substrate would require different stabilising interactions with the enzymes' active sites. Structural analysis of the enzymes could provide insight into the mechanism of these fascinating cyclases.

5.3. Decalins in fungal polyketides

Similar to the aforementioned solanapyrone synthase Sol5 (Section 4.1.), several fungal [4+2] cyclases transform the polyunsaturated products of partially reducing, modular polyketide synthases into decalins.[50–55] Most of the precursor molecules, in contrast to prosolanapyrone II (**5**), carry an activating carbonyl in the dienophile already in the correct oxidation state. For instance, enzymes LovB and LovC from the lovastatin producing *Aspergillus terreus* were attributed to a pathway including a decalin forming stereoselective Diels-Alder step (Scheme 3B).[56] LovB is an iterative polyketide megasynthase with multiple subunits, whilst LovC is a separate accessory protein which catalyses a key enoyl reduction step in the biosynthesis. In the absence of LovC, purified LovB forms pyrone products. The LovC protein is proposed to complex strongly to LovB. With substrate analogue **18** probing the Diels-

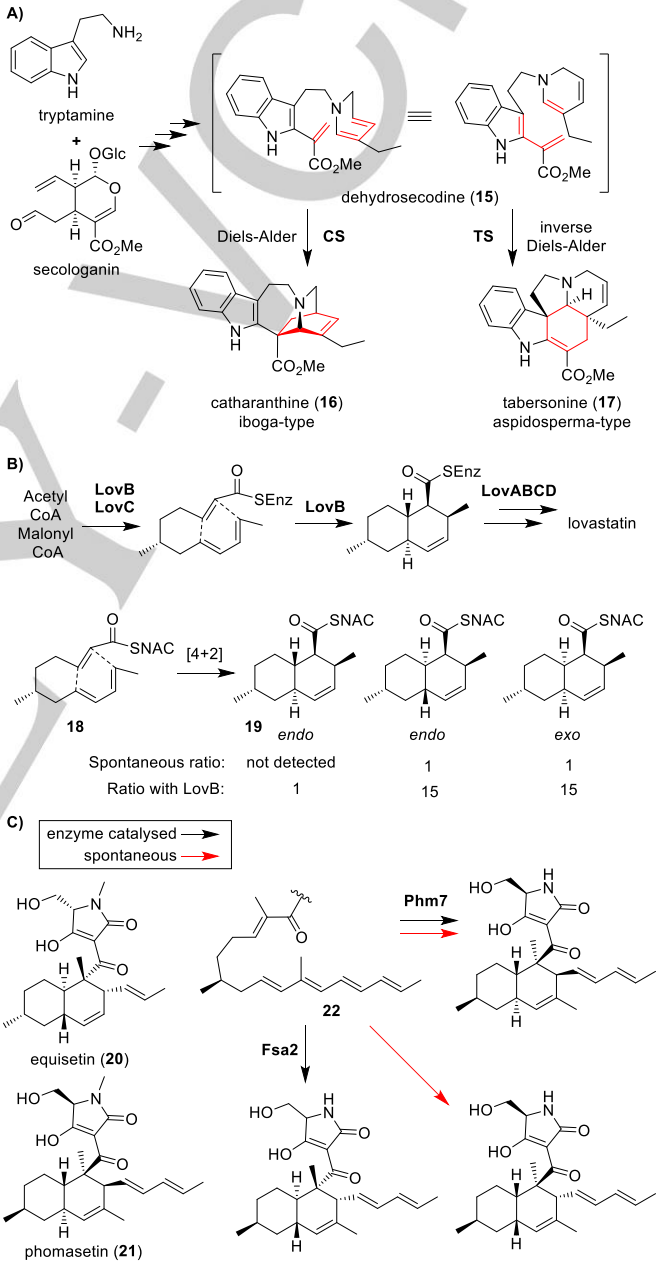

Scheme 3. Examples for how enzymes direct the stereochemical course of [4+2] cycloadditions in **A**) catharanthine and tabersonine, **B**) lovastatin, and **C**) phomasetin and equisetin biosynthesis.

10.1002/chem.201805412

Alder step, LovB shifts the product outcome in favour of the lovastatin-like product **19**, but only to an underwhelming fraction of 4 %. The substrate analogue might not be ideal, or the non-enzymatic reaction dominates the outcome. The proposed transition-states of the Diels-Alder products show that for both the spontaneous products, the C-6 methyl is positioned in a pseudo equatorial position, whilst this methyl would occupy a more hindered pseudo-axial position in the enzyme product. To achieve this selectivity, LovB would have to confine the ligand into the correct conformation for the product to form, possibly through van-der-Waals and steric interactions.

A family of enzymes unrelated to Sol5 or LovB forms decalins in fungal polyketide-nonribosomal peptide hybrids.[50,51,53–55,57] Astonishingly, homologous [4+2] cyclases Fsa2[55] and Phm7 generate the decalin natural products equisetin (**20**) and phomasetin (**21**) with opposite configurations at all chiral centres (Scheme 3C).[51] Both *trans*-decalin configurations differ from the spontaneous *cis*-decalin product. When integrated into an Phm7 knock-out strain, Fsa2 also acted on the slightly longer phomasetin precursor **22** with equisetin chirality, demonstrating the potential of decalin synthases for pathway engineering.[51] As purified protein, Fsa2 was used in the chemoenzymatic synthesis of equisetin (**20**) with perfect stereoselectivity which chemical cyclisation failed to achieve.[57] Relatively high k_{cat} values measured both for Fsa2 (5.8 s^{-1})[57] and related MycB (0.9 s^{-1})[53] certainly benefit such biocatalytic applications.

Another homolog, PvhB, has recently been shown to use “carboxylative deactivation” as a strategy directly opposed to the triggering reactions discussed in Section 4.[58] By installing a carboxylate conjugated with the diene, nonenzymatic formation of the *trans*-decalin is suppressed and PvhB promotes generation of the *cis*-decalin instead.

6. Controlling reaction trajectories

Engineering or designing enzyme activity is most effective when the mechanism is well understood. A full understanding of mechanism ideally involves a combination of experimental and computational analyses, and the two enzymes described in this section, SpnF and LepI, have been investigated using both approaches. Computational analysis of their mechanisms suggests both enzymes catalyse reactions across an energy landscape featuring multiple possible mechanisms and ‘ambimodal’ transition states, in which the reaction trajectory bifurcates to two different products. However, in both cases, a single product is ultimately preferred - a phenomenon compellingly referred to as a case of ‘all roads lead to Rome’.[59]

6.1. Spinosyn A bioynthesis

SpnF, from spinosyn A biosynthesis (Scheme 4A), catalyses a transannular [4+2] cycloaddition, contributing a rate enhancement of approximately 500-fold (k_{cat} = 14 min^{-1} versus k_{non} = 0.03 min^{-1}). SpnF does not alter the stereochemical course of the reaction: the non-enzymatic and SpnF-catalysed reactions have identical stereochemical outcomes.[60]

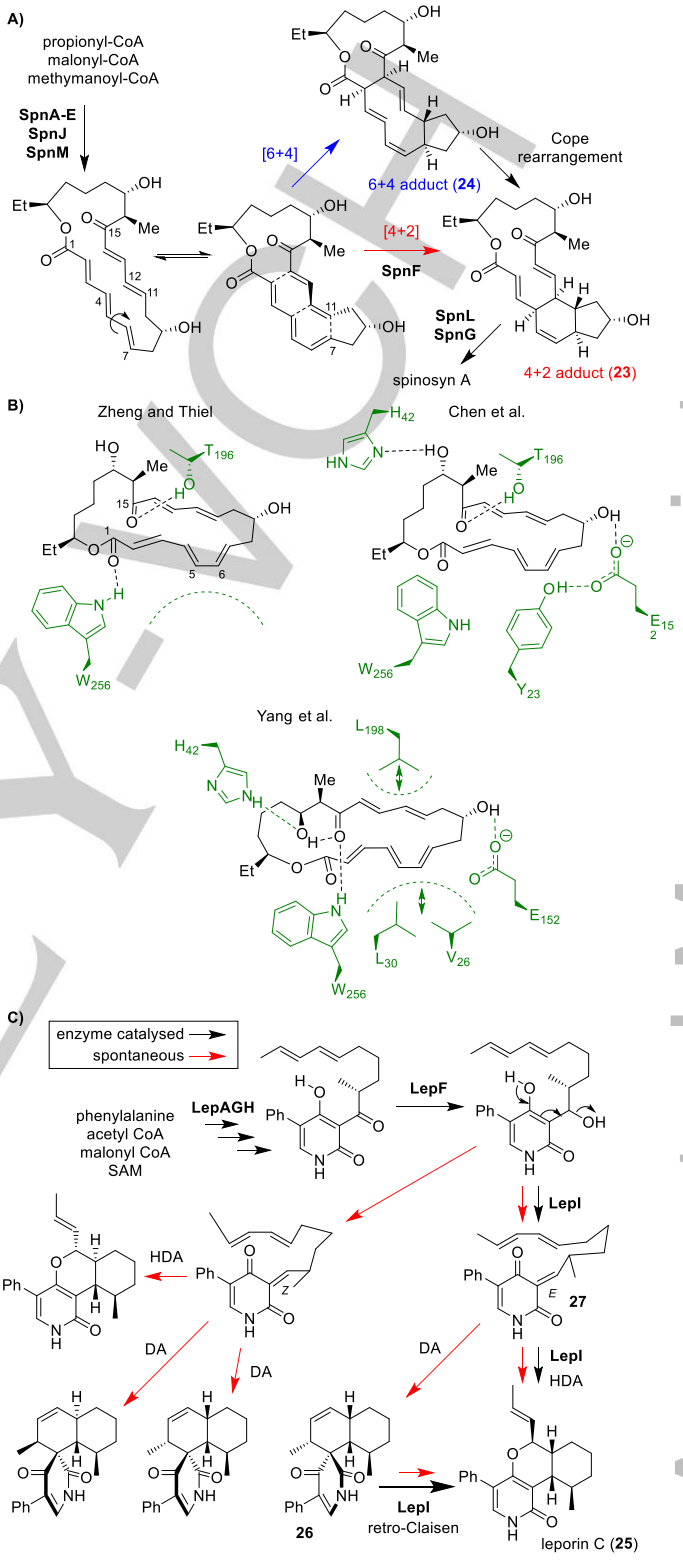

Scheme 4. A) SpnF in spinosyn A biosynthesis apparently favours a [4+2] over a [6+4] cycloaddtion. **B**) Computational studies by Chen et al.,[61] Zheng and Thiel[62] and Yang et al.[63] suggest slightly different catalytic contributions of SpnF. **C**) LepI stears the reaction towards leporin C preferentially via a hetero-Diels-Alder pathway.

10.1002/chem.201805412

Mechanistic analyses of the methyltransferase homologue SpnF are based on a structure with an SAH co-factor, but no other ligand bound. The role of SAH appears to be primarily structural, and accordingly, mutations in the cofactor binding region typically result in denaturation.[60,64]

There have been extensive computational investigations into the SpnF catalysed reaction utilising multiple approaches (Scheme 4B).[61–63,65–68] These simulations are based on the SpnF crystal structure and computational docking[64] and show multiple mechanisms in the gas-phase leading to the [4+2] product **23**. Alongside the direct route via a concerted [4+2] transition state, Patel et al.[67] proposed an alternative route via [6+4] intermediate **24** which undergoes a Cope rearrangement to reveal the [4+2] product **23**. Furthermore, they propose that the initial transition state is ambimodal and able to lead to either [4+2] or [6+4] adducts.

Three groups found no evidence of the [6+4] mechanism in simulated, enzyme-catalysed reaction trajectories (Scheme 4B). Zheng and Thiel[62] propose that rate enhancement was primarily due to an H-bond between Thr196 and the C15 carbonyl, causing electron density withdrawal and increased reactivity of the dienophile. They also suggest that the enzyme favours adoption of the s-*cis* C5-C6 substrate diene conformation necessary for cycloaddition, possibly aided by Trp256 H-bonding the C1 carbonyl. In addition to these factors, Chen et al.[61] propose π-π stacking interactions between the substrate and residues Tyr23 and Trp256 which help position the substrate into a reactive conformation.

The [4+2] mechanism suggested by Yang et al.[63] is remarkably different in the proposed nature of catalysis (Scheme 4B). The Thr196 C15 carbonyl H-bond is absent as the transition state preferentially forms an intramolecular interaction. Instead, H-bonds are present between the transition state and His42, Glu152 and Trp256, decreasing the reaction energy barrier. Most remarkably, the authors suggest that the trajectory over the ambimodal transition state is determined by kinetic energy transfer from hydrophobic residues (Val26, Leu30 and Leu198) to the substrate via femtosecond scale vibrational collisions. This radically dynamic view of enzyme catalysis could be significant in enzymes beyond Diels-Alderases.

Investigation into the enzyme via kinetic isotope effects supports aspects of the computational mechanisms[69] such as the asynchronous formation of the C7-C11 bond prior to the C4-C12 bond.[65,67] Mutational analysis of SpnF could verify the proposed roles of active site residues, but unfortunately such experiments have so far been hindered by a lack of enzyme stability.[60,64] Other experimental targets may include solving structures with substrate or substrate analogues bound and determining definitively whether SAM or SAH is the *in vivo* co-factor. Investigating the presence of the [6+4] mechanism is experimentally challenging as the Cope rearrangement will always lead to the [4+2] product **23**. Design of novel substrates may allow this fascinating proposition to be examined.

6.2. Leporin C biosynthesis

A remarkably similar ambimodal pericylic transition state has also been proposed for the LepI cyclase, though in this instance the energy landscape, which includes a stable intermediate, allows the system to be more experimentally tractable.[70] The biosynthesis of leporin C (**25**), a cytotoxic hybrid PKS-NRPS natural product from *Aspergillus*, involves pericyclic steps catalysed by the stand-alone enzyme LepI.[70] Formation of a stable ketone intermediate by LepA, G and H is followed by reduction catalysed by LepF, a short-chain dehydrogenase, generating a secondary alcohol. In the absence of LepI this compound can spontaneously dehydrate, leading to the formation of quinone methide stereoisomers which then undergo Diels-Alder (DA) or hetero-Diels-Alder (HDA) cyclisations to form a mixture of adducts (Scheme 4C, red arrows). When LepI was included in the reaction, only two products were observed: the major product leporin C (**25**), the *E*-HDA-adduct, and lower quantities of the *E*-DA-adduct **26**, which over time was converted into leporin C (**25**). Experimentally, LepI was observed to catalyse stereoselective dehydration to yield the *E*-methide intermediate **27**, which is crucial for establishing the ultimate product stereochemistry. The enzyme was found to promote formation of the HDA-adduct **25** compared to the DA-adduct **26** (1:1 with LepI, 94:6 without LepI). Furthermore, LepI can then catalyse a retro-Claisen rearrangement of **26**, converting it into **25**. This is the first reported enzyme catalysing a retro-Claisen rearrangement, and the reaction was catalysed with an impressive rate enhancement of 1.8×10^5 (k_{cat} versus k_{non}).

In a similar manner to SpnF, LepI has sequence homology to O-methyl-transferases and utilises SAM as a co-factor, despite no methylation steps appearing in the leporin biosynthesis. Experiments with SAM, SAH and the charged mimic sinefungin established that the positively charged co-factor was important for both dehydration and retro-Claisen activities. Computational DFT analysis indicates that the initial (hetero) Diels-Alder step is controlled by an ambimodal transition state, and the enzyme shifts the post-transition state bifurcation to favour direct production of the HDA adduct **25**. Furthermore, the analysis also supports the role of the SAM positive charge in lowering the energy of the ambimodal and retro-Claisen transition states.

A recently published structure of LepI in complex with SAM has provided insight into the mechanism of this multifunctional enzyme.[71] Computational docking of substrates indicate residues H133 and D296 are involved in the dehydration step, whilst the selectivity of the pericyclic reactions is a result of conformational restraints provided by hydrophobic residues. The preferred pose of the docked intermediate **27** is more conducive to HDA rather than DA cyclisation, which supports the empirically measured enzyme selectivity. Further structural and mutational investigations of this fascinating enzyme will provide further insight into the role of SAM and how its various activities are coupled. This system is ideal for investigation of enzymatic ambimodal cycloaddition transition states since both products can be identified.

10.1002/chem.201805412

7. Putting the lid on an entropy trap

Coercing reaction partners into a conformation leading to a desired cycloaddition comes at a high entropic cost[5] which the enzyme should reduce for effective catalysis. How is this achieved? Catalytic champions among the natural [4+2] cyclases are the enzymes involved in tetronate and tetramate formation in the abyssomycin, versipelostatin and pyrridomycin biosynthesis.[13,72,73] The 4 x 10^4-fold rate acceleration observed with AbyU from abyssomycin synthesis,[73] comparable in magnitude to the Lewis acid catalysis with aluminum trichloride, and the transition state affinity of 3.9 x 10^8 M^{-1} (catalytic proficiency, $[k_{cat}/K_M]/k_{uncat}$)[15] are excellent for a cyclase. Interestingly, most of the outstanding efficiency appears to be not owed to individual catalytic residues but to the cooperative action of multiple residues in a lid covering the active site.[74]

The structure of PyrI4 from pyrridomycin synthesis with product bound has illuminated details of the reaction mechanism (Figure 1A).[74] Although Gln115 and His117 are close to the carbonyl group of the dienophile, they show little mutational sensitivity. In the Gln115Ala mutant, k_{cat} only drops by a factor of three and remains unchanged in the His117Ala mutant. However, removal of an N-terminal helix covering the active site and mutation of individual salt bridge forming residues in this helix abolishes activity (Figure 1A). The N-terminal lid apparently holds the transition state tight in the active site but then quickly releases the product. Comparable lid-like movements have been predicted for AbyU, a homologue of PyrI4. Discrimination of the fine differences between transition state and product combined with a dynamic release mechanism might be key to efficient entropy trapping in [4+2] cyclases. Lid closure might force the substrate into the reactive conformation in an induced-fit like mechanism and thus reduce the entropy of activation.

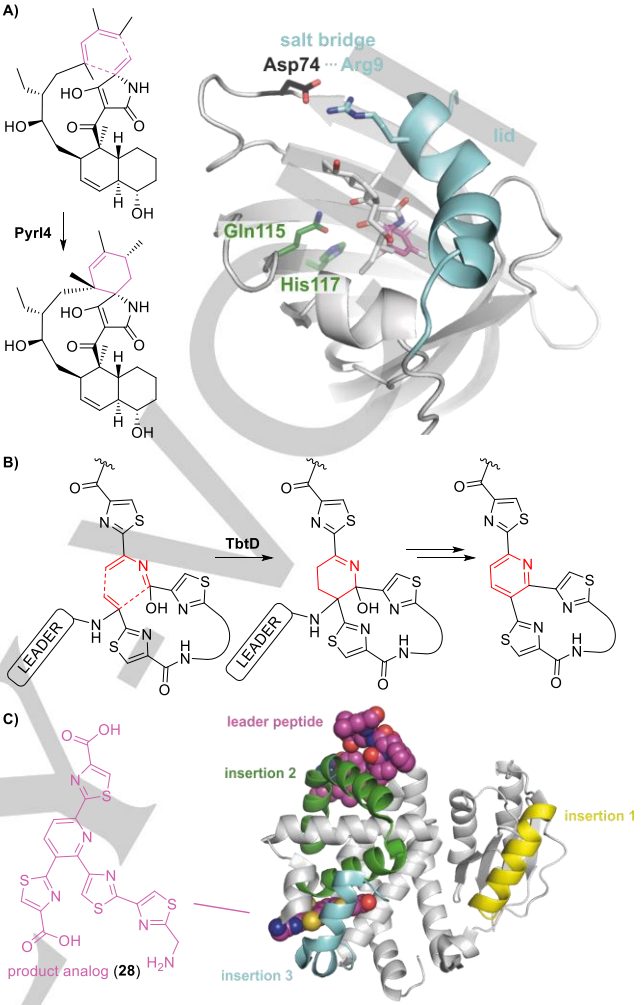

Figure 1. A) In PyrI4, a salt bridge (sticks in black and cyan) holding a lid in place (cartoon in cyan), but far distant from the cycloaddition reaction (ring highlighted in pink), is highly sensitive to mutation. Binding pocket residues Gln115 and His117 (green sticks) are insensitive to mutation. The structure of PyrI4 in complex with product (PDB code 5BU3) has been rendered in Pymol.[74] **B**) Reaction catalysed by pyridine synthase TbtD. **C**) Structure of PbtD (PBD code 5W99) in complex with product analog **28** and overlayed with the leader peptide from the homologous structure of TbtD (PDB code 5WA4). Both ligands are shown as pink spheres.

8. Leading peptides to cyclisation

In the induced fit mechanism described above, substrate binding and catalysis are intimately coupled, but binding and catalysis can also occur at distinct locations in the enzyme structure. Ribosomal peptide natural products (RiPPs) are appended with cleavable leader peptides as universal binding handles to recruit various enzymes to work on the peptide backbone. Since the leader peptide guarantees binding, structural modifications are well tolerated in the core peptide, which has been exploited for combinatorial biosynthesis.[75] This enzymatic strategy, in which binding and catalysis are separated, seems to make RiPPs highly evolvable.

Pyridine synthases like TbtD have the unique ability to introduce pyridine residues into RiPPs via an aza-cycloaddition reaction.[76–79] In the case of the antibiotic thiomuracin, dehydration of two serine residues to dehydroalanine in the precursor peptide prepares for the pyridine synthase reaction catalyzed by TbtD (Figure 1B). The dienophile is the first residue of the core peptide and the diene partner is presumably generated by tautomerization of a downstream dehydroalanine to an iminol. After cycloaddition, pyridine formation is completed by dehydration and elimination of the leader peptide.

Structurally, three insertions make the difference between related, non-cyclizing dehydration elimination domains and the pyridine synthase TbtD.[76] One structure in complex with the leader peptide shows it to interact with the second insertion. Another structure in complex with truncated pyridine product **28** shows its binding at the third insertion (Figure 1C). Ligand binding enhances the structural order in the third insertion, perhaps indicating an induced-fit like mechanism similar to the one observed with the aforementioned lid. The leader peptide binds to the enzyme with a low micromolar dissociation constant and its absence abolishes

10.1002/chem.201805412

binding and reactivity.[76,78,79] In addition to the leader peptide, pyridine synthases require C-terminal recognition elements, possibly to distinguish between multiple potential dehydroalanine reaction partners.[78] Knowledge of the recognition elements enables the biocatalytic application of pyridine synthases on un-natural, possibly synthetic peptide substrates.[78,80] Still mostly in the dark, however, are catalytic details regarding the [4+2] cycloaddition.

9. Polar, bimolecular and stepwise

Intermolecular reactions render a synthesis convergent and thus break one large synthetic problem down into several small ones. One iconic example from total synthesis illustrating the utility of intermolecular, asymmetric Diels-Alder reactions is Liu and Jacobsen's synthesis of the antifungal natural product ambruticin.[81] They employed Diels-Alder reactions under control of a chiral chromium catalyst to assemble two pyran rings at both ends of the molecule. Hence, intermolecular cycloaddition reactions are particularly valuable in total synthesis for the build-up of complex scaffolds. Yet, almost all natural [4+2] cyclases known today have only been shown to promote intramolecular reactions. In nature, rare examples of intramolecular cycloaddition catalysts are riboflavin synthase and macrophomate synthase.

9.1. Riboflavin synthase

Riboflavin synthase catalyses an intermolecular cyclisation reaction that is part of primary metabolism and should therefore be old on an evolutionary time scale. This reaction leads to the biosynthesis of the essential cofactor riboflavin via pentacyclic intermediate **29** (Figure 2A).[82,83] Several mechanisms have been proposed for the riboflavin synthase catalysed dimerisation of 6,7-dimethyllumazine **30** but DFT calculations in water have ruled out most of them.[84] Among the energetically disfavoured routes were a radical tautomerization followed by step-wise cyclization and hydride transfer followed by Diels-Alder cyclization.[84,85] The mechanism favoured on computational grounds and compatible with kinetic isotope effects[86] involves a tautomerization of one reaction partner to diene-diamine **31** and sequential nucleophilic additions of the 6- and 7-methylene groups to the 7- and 6-carbons of the other reaction partner.

The proposed riboflavin synthase mechanism is so appealing because only acid-base chemistry is required - a speciality of enzymes. Several transition states might be relevant for catalysis. Those leading to C-H deprotonation of the 6- and 7-methyl groups cause large deuterium isotope effects of 5 and 1.3-fold, respectively.[86] Computation predicts both carbon-carbon bond formation events to be energetically relevant too, with activation energies in the range of 20 kcal/mol. Both barriers are lowered when the electrophilic reactant is protonated at one of the nitrogen atoms.

Calculations of the Gibbs energy profile were conducted in water, so participation of enzyme side chains could not be accurately predicted. However, an earlier crystal structure with substrate

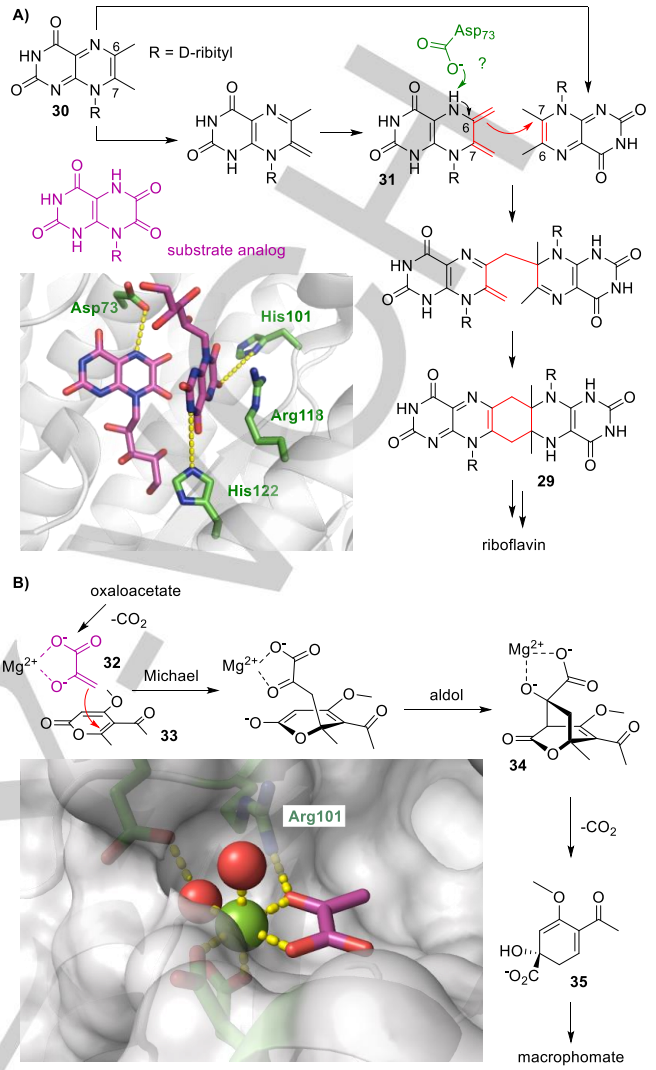

Figure 2. A) Proposed mechanisms of the reaction catalysed by riboflavin synthase[84] and active site structure of the enzyme from *M. jannaschii* (PDB code 2B99).[87] The bound substrate analogs are shown as pink, and selected polar, conserved active site residues as green sticks. **B**) Presumable reaction mechanism catalysed by macrophomate synthase. The structure of macrophomate synthase (PDB code 1IZC)[88] is shown in complex with enolpyruvate as a ligand (pink sticks; water: red spheres; Mg^{2+}: green sphere; active site residues: green sticks).

analogue bound[87] shows residues conserved among archaeal enzymes that might function as proton transfer catalysts (Figure 2A). Asp73, for instance, is suggestively positioned to participate in the first C-C bond formation.[87] Proximity of residue Cys76 to the ligands raises the possibility of additional nucleophilic catalysis but this residue is not strictly conserved.[84,87]

9.2. Macrophomate synthase

Another example of an intermolecular cyclase is the fungal enzyme macrophomate synthase.[88–91] This enzyme catalyses a

10.1002/chem.201805412

net-cycloaddition between enolpyruvate (**32)** and 2-pyrone **33** (Figure 2B). However, the cycloaddition product **34** is not directly detectable as it undergoes immediate decarboxylation to the known intermediate **35**, which then dehydrates non-enzymatically to reveal macrophomate.[90] There are multiple indications that the initial enzyme-catalysed cyclisation occurs in a step-wise manner rather than via a concerted Diels-Alder mechanism. These include the enzyme's phylogenetic classification as an aldolase, its proven aldolase side-reactivity[91] and QM-MM calculations suggesting a Michael-aldol mechanism.[92]

The proposed step-wise macrophomate synthase mechanism involves the generation of a reactive enolate intermediate which undergoes a 1,6-Michael addition followed by an aldol-ring closure. The presence of an enolate intermediate and Michael addition reaction resembles the mechanism of iridoid synthase (Section 4.2), though in iridoid synthase the addition occurs in the 1,4 position.[34,41,43] Notably, macrophomate synthase also catalyses 1,2-additions of enolpyruvate to a range of aldehyde acceptors with potential synthetic applications.[91] In contrast to the reductive enolate formation in iridoid synthase, macrophomate synthase generates the Michael donor by Mg^{2+} assisted decarboxylation of oxaloacetate to enolpyruvate (**32**).

Participation of the enzyme in the cycloaddition reaction is evident from the enantioselectivity which is probably caused by blocking attack from one face of the enolpyruvate (Figure 2B).[88] Furthermore, structural investigations led to the identification of an arginine residue (Arg101) that could stabilise the negative charge forming on the 2-pyrone during Michael addition. The "dienophile" pyruvate coordinated to the metal centre in a bidentate fashion with one face exposed to the diene resembles the arrangement in chiral catalysts and artificial metalloenzymes (Scheme 1). However, the metal here serves as the electron sink for decarboxylation, not for narrowing the energy gap of a cycloaddition.

To regard [4+2] cyclases with a stepwise mechanism as "failed Diels-Alderases" is probably a mistake. Quantum-mechanical calculations of Diels-Alder reactions with various dienophiles show two trends:[93] (a) more polar reactions involving more charge transfer proceed faster and (b) more polar or even ionic Diels-Alder reactions tend to be less synchronous. Therefore, rate acceleration in Diels-Alderases may be achieved through increasing the polar character of the reaction, which in the extreme would result in a step-wise reaction. By taking a highly polar route to the products via anionic intermediates, macrophomate synthase achieves an overall k_{cat} of 0.6 s^{-1}.[89]

10. Designer cyclases

Enzyme designers aim to meet the need of synthetic chemistry for fast and specific catalysts through the development of tailor-made enzymes. Novel enzymes catalysing cycloadditions have always been a prime target for these approaches. In contrast to current artificial metalloenzymes which embed a metal based cyclisation catalyst in a largely inert scaffold, *de novo* designs have active sites constructed from scratch - usually employing the standard repertoire of proteinogenic amino acids.

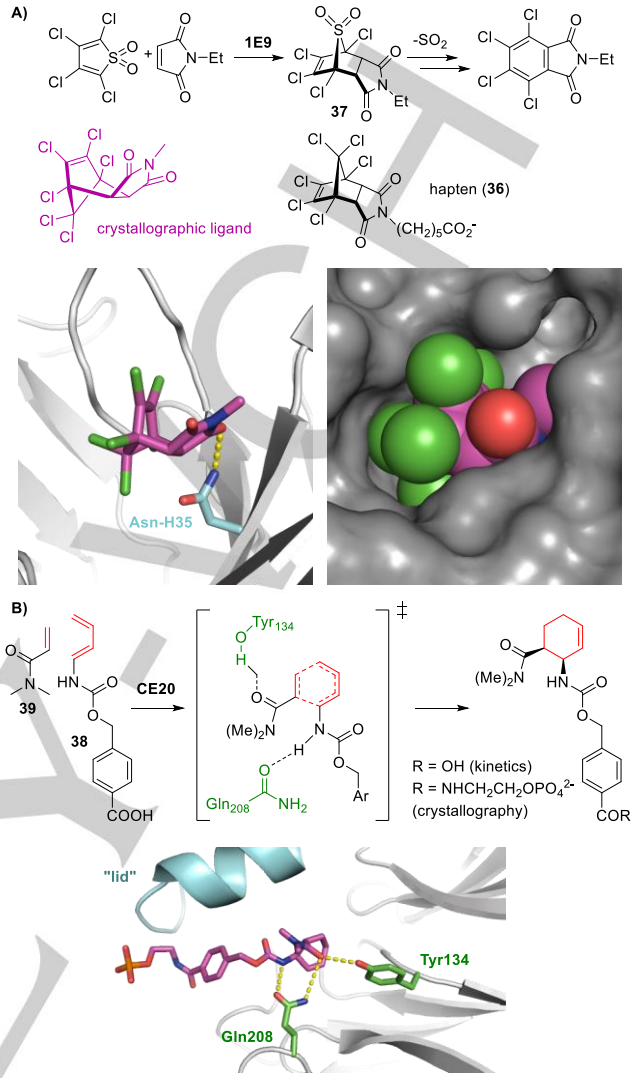

Figure 3. A) Reaction catalysed by Diels-Alderase antibody 1E9. The active site structure (PDB code 1C1E) is shown with a product analog bound in pink (left: sticks; right: spheres), with the protein shown as grey cartoon (left) and surface (right). **B**) A lid-like structure (cyan) has been added to computationally designed and evolved catalyst CE20 (PDB code 4O5T).

10.1. Catalytic antibodies

Catalytic antibodies offer important lessons about cycloaddition catalysis and cyclase design.[94] Before computers became powerful enough to predict transition state and protein active site geometries, raising catalytic antibodies against transition state analogues was a promising strategy for designing enzyme catalysts for unnatural reactions. Despite some initial successes, catalytic antibodies have fallen out of favour because their catalytic efficiencies remained inferior to biological catalysts, possibly due to limitations of the antibody scaffold.[94]

The origins of cycloaddition catalysis have been investigated in detail with catalytic antibody 1E9 raised against hapten **36** (Figure 3A).[2] This designer catalyst shows a catalytic proficiency of 1.4 x

10^7 M^{-1},[94] well in the range of natural [4+2] cyclases. Surprisingly, 1E9 does not act as an entropy trap; whilst the enthalpy of activation determined from the temperature dependence of k_{cat} is lowered by 4.2 kcal/mol, the entropy of activation remains equally unfavourable for the catalysed and uncatalyzed reaction (-22.1 and -21.5 cal mol^{-1} K^{-1}, respectively).[95] According to molecular dynamics simulations, residue Asn-H35 is crucial for the enthalpic effect as it hydrogen bonds to the carbonyl oxygen of the dienophile more strongly in the transition state than in the ground state. The catalytic interaction is bolstered by the hydrophobic environment with perfect shape complementarity to the transition state (Figure 3A). Product inhibition, a possible side-effect of strong transition state binding in Diels-Alderases, is avoided here through elimination of sulphur dioxide from product **37**.

10.2. Computational design

For designer enzymes to become relevant for chemical synthesis, we must develop computational methods to design them in a short amount of time and with a high level of accuracy.[96] A computational cyclase design from the Baker lab, DA_20_00,[97] employs a glutamine and a tyrosine side chain interaction with the diene **38** and the dienophile N,N-dimethylacrylamide (**39**; Figure 3B), but only reaches a catalytic proficiency of 8.7 x 10^3 M^{-1}. Subsequent optimization by cassette mutagenesis and error-prone PCR has yielded DA_20_20 with a 620-fold higher catalytic proficiency due to a 45-fold improved k_{cat} and slightly improved K_M values (3.5 and 3.9-fold for the diene and dienophile respectively).[97,98] Installation of a computationally designed lid covering the active site and subsequent evolutionary optimization increased the catalytic proficiency to 8.4 10^7 M^{-1},[98,99] only 5-fold below the natural best-in-class AbyU discussed above (Section 7). The resulting catalyst CE20 (Figure 3B) displays the excellent stereoselectivity expected from a tightly tailored enzyme binding pocket. At present, the high demand for time and manpower make *de novo* enzyme design approaches unpracticable for biocatalytic applications. However, the astonishing accuracy of the CE20 design and the growing reliability of the underlying in silico and in vitro optimisation protocols hold great promise for the future.

11. Discussion

11.1. Cyclases: a patchwork family

With a range of natural [4+2] cyclases now identified and some of them characterised in detail, the question can be asked: how do they evolve and why does this process appear so rare? With the exception of riboflavin synthase, which catalyses a reaction in primary metabolism, [4+2] cyclases seem to have appeared relatively late in evolution: the enzymes are phylogenetically highly diverse without any apparent sequence relation between the different classes, and each class occurs in a small group of organisms as part of a specialised/secondary metabolic pathway (Table 1). The cyclase classes appear to have evolved independently to solve very specific metabolic questions, and consequently [4+2] cyclases have evolved multiple times from a wide range of unrelated enzymes, including redox enzymes, aldolases, and polyketide synthases.

One of the most proficient [4+2] cyclases, AbyU, is a small beta barrel with only 141 residues. If small and efficient [4+2] cyclases can exist, why did cycloaddition reactions not become more widespread early in evolution? Perhaps the limiting factor is not the evolution of the cyclase but rather the presence of suitable substrates. For a [4+2] cycloaddition to proceed, diene, dienophile and, usually, at least one conjugated functional group for electronic activation must preexist in a spatial arrangement permissive for reaction. A search in the *Escherichia coli* metabolome comprising 3,760 metabolites, for instance, reveals only a few all-carbon dienes mostly related to aromatic amino acid metabolism and a few compounds which might be erroneously assigned to *E. coli* metabolism (retinal, leukotriene).[100] There are limited opportunities for a novel [4+2] cyclase to emerge in this model organism and likely in many other species. Therefore, it seems that the rarity of cyclases is a consequence of the rarity of the requisite diene and dienophile systems.

Table 1. Updated classification of natural [4+2] cyclases.[9]

[4+2] Cyclase class	Example enzymes	Ancestral family
Polyene cyclase	LovB/C	Polyketide synthase
	Sol5	FAD dependent oxidase
	PyrE3	FAD dependent oxidase
	SpnF	SAM dependent methyltransferase
	MycB, Fsa2, CghA, UcsH, PvhB	Lipocalin
Riboflavine synthase		unknown
Spirotetronate/-tetramate synthase	AbyU, PyrI4	unknown
Pyridine synthase	TclM, TbtD, PbtD	Lanthipeptide dehydratase elimination domain
Macrophomate synthase	MPS	Malate synthase
Iridoid synthase	CrISY, AmISY, NEPS	Short chain dehydrogenase
Catharanthine/tabersonine synthase	CS, TS	α/β-Hydrolase

11.2. Stabilizing or chaperoning the transition state

Fundamental, physico-chemical limitations of [4+2] cycloaddition catalysis could also hinder cyclase evolution. Both natural enzymes and designer catalysts tend to be sluggish catalysts in terms of rate acceleration (k_{cat}/k_{uncat}) and catalytic proficiency ($[k_{cat}/K_M]/k_{uncat}$; Table 2) compared to some enzymes from primary metabolism with proficiencies up to 2.0 10^{23} M^{-1}.[15] In cases where uncatalyzed cyclization rates are fast but undesired products are present, e.g. in iridoid biosynthesis, the enzyme active site could mostly act as a chaperone for the transition state, similar to the dirigent proteins proposed to exert stereochemical influence in lignan biosynthesis.[101] Rather than lowering the energy of the cycloaddition transition state, as one would expect a typical enzyme to do, these 'chaperone' proteins may instead bias the reaction trajectory by other means. For example, they may destabilise undesired reaction trajectories, which in effect can lead to reaction selectivity without stabilisation of a transition state (i.e. negative catalysis). Other proteins may exert dynamic control of bifurcation following ambimodal transition states (e.g. SpnF, LepI) which can bias a reaction outcome without necessarily increasing reaction rate.

Table 2. Catalytic efficiency parameters of selected [4+2] cycloaddition catalysts.

Catalyst	Type	$1/K_{TS}$ (M^{-1})[a]	k_{cat}/k_{uncat}[b]	Reference
$AlCl_3$	Small molecule	not applicable	~ 1 10^5	[102]
1E9	Antibody	1.4 10^7	1.0 10^3 M	[95]
CE20	Designer enzyme	8.4 10^7	4.8 10^2 M	[98]
SpnF	Natural enzyme	4 10^6	5 10^2	[60]
AbyU	Natural enzyme	3.9 10^8	4.0 10^4	[73]
PvhB	Natural enzyme	1.7 10^8	9.4 10^4	[58]

[a] Defined as $(k_{cat}/K_M)/k_{uncat}$ for intramolecular or $k_{cat}/(K_{M1}\ K_{M2})/k_{uncat}$ for intermolecular reactions.[15] [b] The rate acceleration k_{cat}/k_{uncat} is not directly comparable between mono- and bimolecular reactions, for which the constant is unitless or given in M, respectively.

Two effects might explain the poor transition state binding of cyclases. First, the proximity effect for rather hydrophobic substrates is already high in water and cannot be fully exploited for enzyme catalysis.[22] Second, the similarity between the transition state and the products renders selective transition state stabilization difficult.[103] In particular, the potential for one of the most important enzyme functions, electrostatic preorganization,[104] might be low in reactions with hydrophobic partners. These limitations notwithstanding, a cyclase with a rate acceleration of 10^4 fold combined with enzyme-like selectivity can still be tremendously useful for biocatalysis.

12. Outlook

Exciting discoveries of natural [4+2] cyclases have encouraged a growing number of researchers to sift through biosynthetic pathways to find new members of this diverse family of enzymes. Many [4+2] cyclases are likely still awaiting discovery, but not every search will be rewarded with a new enzyme - some biological cyclisation reactions proceed without a catalyst.[105] Finding more bimolecular [4+2] cyclases, which are suspected in a number of pathways,[106] would be desirable in particular because of their potential synthetic utility.

Cycloadditions are more widely used in chemical synthesis than in biosynthesis. Therefore, there is a demand for [4+2] cyclases that nature may not be able to fulfil. Enzyme engineers are working hard to expand the toolkit of organic chemists with efficient, tailor made cyclases. Great potential seems to reside in artificial metalloenzymes, which could possibly reach the efficiencies of typical, natural enzymes if they were subjected to extensive genetic optimization.[31] A growing number of natural and designed [4+2] cyclases will hopefully become available in the years to come and finally equip one of the most important reactions in synthetic chemistry with versatile biocatalysts.

Acknowledgements

This work was kindly supported by grants of the European Research Council (311363), BBSRC (BB/J004561/1) to S.E.O and a Daimler und Benz fellowship (H.K.). B.L. acknowledges funding from UK Biotechnological and Biological Sciences Research Council (BBSRC) and Engineering and Physical Sciences Research Council (EPSRC) joint-funded OpenPlant Synthetic Biology Research Centre (BB/L014130/1). We thank Dr. Lorenzo Caputi for helpful discussions.

Keywords: Diels-Alderase • [4+2] cyclase • biocatalysis • enzyme mechanism • enzyme design

[1] O. Diels, K. Alder, *Justus Liebig's Ann. der Chemie* **1928**, *460*, 98–122.

[2] D. Hilvert, K. W. Hill, K. D. Nared, M. T. M. Auditor, *J. Am. Chem. Soc.* **1989**, *111*, 9261–9262.

[3] A. C. Bazan, J. M. Edwards, U. Weiss, *Tetrahedron* **1978**, *34*, 3005–3015.

[4] H. Oikawa, K. Katayama, Y. Suzuki, A. Ichihara, *J. Chem. Soc., Chem. Commun.* **1995**, 1321–1322.

[5] J. Sauer, R. Sustmann, *Angew. Chem. Int. Ed.* **1980**, *19*, 779–807.

[6] R. Huisgen, *Angew. Chem. Int. Ed.* **1968**, *7*, 321–328.

[7] B. S. Jeon, S. A. Wang, M. W. Ruszczycky, H. Liu, *Chem. Rev.* **2017**, *117*, 5367–5388.

[8] C. T. Walsh, Y. Tang, *Biochemistry* **2018**, *57*, 3087–3104.
[9] A. Minami, H. Oikawa, *J. Antibiot. (Tokyo).* **2016**, *69*, 500–506.
[10] K. Klas, S. Tsukamoto, D. H. Sherman, R. M. Williams, *J. Org. Chem.* **2015**, *80*, 11672–11685.
[11] H. J. Kim, M. W. Ruszczycky, H. Liu, *Curr. Opin. Chem. Biol.* **2012**, *16*, 124–131.
[12] C. S. Jamieson, M. Ohashi, F. Liu, Y. Tang, K. N. Houk, *Nat. Prod. Rep.* **2018**, DOI 10.1039/C8NP00075A.
[13] Q. Zheng, Z. Tian, W. Liu, *Curr. Opin. Chem. Biol.* **2016**, *31*, 95–102.
[14] W. L. Kelly, *Org. Biomol. Chem.* **2008**, *6*, 4483–4493.
[15] A. Radzicka, R. Wolfenden, *Science* **1995**, *267*, 90–93.
[16] E. M. Carreira, L. Kvaerno, *Classics in Stereoselective Synthesis*, Wiley-VCH, Weinheim, **2009**.
[17] K. Ishihara, A. Sakakura, *Compr. Org. Synth. II* **2014**, *5*, 351–408.
[18] R. Brückner, *Reaktionsmechanismen*, Springer Spektrum, Berlin, Heidelberg, **2004**.
[19] E. J. Corey, *Angew. Chem. Int. Ed.* **2002**, *41*, 1650–1667.
[20] F. Schwizer, Y. Okamoto, T. Heinisch, Y. Gu, M. M. Pellizzoni, V. Lebrun, R. Reuter, V. Köhler, J. C. Lewis, T. R. Ward, *Chem. Rev.* **2018**, *118*, 142–231.
[21] D. A. Evans, S. J. Miller, T. Lectka, P. von Matt, *J. Am. Chem. Soc.* **1999**, *121*, 7559–7573.
[22] R. Breslow, *Acc. Chem. Res.* **1991**, *24*, 159–164.
[23] A. B. Smith, N. J. Liverton, N. J. Hrib, H. Sivaramakrishnan, K. Winzenberg, *J. Am. Chem. Soc.* **1986**, *108*, 3040–3048.
[24] M. Uroos, P. Pitt, L. M. Harwood, W. Lewis, A. J. Blake, C. J. Hayes, *Org. Biomol. Chem.* **2017**, *15*, 8523–8528.
[25] J. R. McCabe, C. A. Eckert, *Acc. Chem. Res.* **1974**, *7*, 251–257.
[26] H. F. Chow, C. C. Mak, *J. Org. Chem.* **1997**, *62*, 5116–5127.
[27] M. T. Reetz, N. Jiao, *Angew. Chem. Int. Ed.* **2006**, *45*, 2416–2419.
[28] T. K. Hyster, T. R. Ward, *Angew. Chem. Int. Ed* **2016**, *55*, 2–16.
[29] M. Jeschek, R. Reuter, T. Heinisch, C. Trindler, J. Klehr, S. Panke, T. R. Ward, *Nature* **2016**, *537*, 661–665.
[30] J. Bos, F. Fusetti, A. J. M. Driessen, G. Roelfes, *Angew. Chem. Int. Ed.* **2012**, *51*, 7472–7475.
[31] C. Zeymer, D. Hilvert, *Annu. Rev. Biochem.* **2018**, *87*, 131–157.
[32] K. Kasahara, T. Miyamoto, T. Fujimoto, H. Oguri, T. Tokiwano, H. Oikawa, Y. Ebizuka, I. Fujii, *ChemBioChem* **2010**, *11*, 1245–1252.
[33] H. Oikawa, T. Kobayashi, K. Katayama, Y. Suzuki, A. Ichihara, *J. Org. Chem.* **1998**, *63*, 8748–8756.
[34] F. Geu-Flores, N. H. Sherden, V. Courdavault, V. Burlat, W. S. Glenn, C. Wu, E. Nims, Y. Cui, S. E. O'Connor, *Nature* **2012**, *492*, 138–42.
[35] F. Alagna, F. Geu-Flores, H. Kries, F. Panara, L. Baldoni, S. E. O'Connor, A. Osbourn, *J. Biol. Chem.* **2016**, *291*, 5542–5554.
[36] N. H. Sherden, B. Lichman, L. Caputi, D. Zhao, M. O. Kamileen, C. R. Buell, S. E. O'Connor, *Phytochemistry* **2018**, *145*, 48–56.
[37] B. Xiang, X. Li, Y. Wang, X. Tian, Z. Yang, L. Ma, X. Liu, Y. Wang, *Molecules* **2017**, *22*, 1387.
[38] H. Kries, F. Kellner, M. O. Kamileen, S. E. O'Connor, *J. Biol. Chem.* **2017**, *292*, 14659–14667.
[39] B. R. Lichman, M. O. Kamileen, G. R. Titchiner, G. Saalbach, C. E. M. Stevenson, D. M. Lawson, S. E. O'Connor, *Nat. Chem. Biol.* **2019**, *15*, 71–79.
[40] Y. Hu, W. Liu, S. R. Malwal, Y. Zheng, X. Feng, T. Ko, C.-C. Chen, Z. Xu, M. Liu, X. Han, et al., *Angew. Chem. Int. Ed.* **2015**, *54*, 15478–15482.
[41] H. Kries, L. Caputi, C. E. M. Stevenson, M. O. Kamileen, N. H. Sherden, F. Geu-Flores, D. M. Lawson, S. E. O'Connor, *Nat. Chem. Biol.* **2016**, *12*, 6–8.
[42] L. Qin, Y. Zhu, Z. Ding, X. Zhang, S. Ye, R. Zhang, *J. Struct. Biol.* **2016**, *194*, 224–230.
[43] S. Lindner, F. Geu-Flores, S. Bräse, N. H. Sherden, S. E. O'Connor, *Chem. Biol.* **2014**, *21*, 1452–1456.
[44] A. I. Scott, *Bioorg. Chem.* **1974**, *3*, 398–429.
[45] A. I. Scott, C. C. Wei, *Tetrahedron* **1974**, *30*, 3003–3011.
[46] A. I. Scott, *Acc. Chem. Res.* **1970**, *3*, 151–157.
[47] H. Mizoguchi, H. Oikawa, H. Oguri, *Nat. Chem.* **2014**, *6*, 57–64.
[48] L. Caputi, J. Franke, S. C. Farrow, K. Chung, R. M. E. Payne, T. Nguyen, T. T. Dang, I. Soares Teto Carqueijeiro, K. Koudounas, T. Dugé de Bernonville, et al., *Science* **2018**, *360*, 1235–1239.
[49] Y. Qu, M. E. A. M. Easson, R. Simionescu, J. Hajicek, A. M. K. Thamm, V. Salim, V. De Luca, *Proc. Natl. Acad. Sci. USA* **2018**, *115*, 3180–3185.
[50] L. Li, M. C. Tang, S. Tang, S. Gao, S. Soliman, L. Hang, W. Xu, T. Ye, K. Watanabe, Y. Tang, *J. Am. Chem. Soc.* **2018**, *140*, 2067–2071.
[51] N. Kato, T. Nogawa, R. Takita, K. Kinugasa, M. Kanai, M. Uchiyama, H. Osada, S. Takahashi, *Angew. Chem. Int. Ed.* **2018**, *57*, 9754–9758.
[52] Q. Zheng, Y. Gong, Y. Guo, Z. Zhao, Z. Wu, Z. Zhou, D. Chen, L. Pan, W. Liu, *Cell Chem. Biol.* **2018**, *25*, 718–727.e3.
[53] L. Li, P. Yu, M. C. Tang, Y. Zou, S. S. Gao, Y. S. Hung, M. Zhao, K. Watanabe, K. N. Houk, Y. Tang, *J. Am. Chem. Soc.* **2016**, *138*, 15837–15840.
[54] M. Sato, F. Yagishita, T. Mino, N. Uchiyama, A. Patel, Y. H. Chooi, Y. Goda, W. Xu, H. Noguchi, T. Yamamoto, et al., *ChemBioChem* **2015**, *16*, 2294–2298.
[55] N. Kato, T. Nogawa, H. Hirota, J. H. Jang, S. Takahashi, J. S. Ahn, H. Osada, *Biochem. Biophys. Res. Commun.* **2015**, *460*, 210–215.
[56] K. Auclair, A. Sutherland, J. Kennedy, D. J. Witter, J. P. Van Den Heever, C. R. Hutchinson, J. C. Vederas, *J. Am. Chem. Soc.* **2000**, *122*, 11519–11520.
[57] X. Li, Q. Zheng, J. Yin, W. Liu, S. Gao, *Chem. Commun.* **2017**, *53*, 4695–4697.
[58] D. Tan, C. S. Jamieson, M. Ohashi, M.-C. Tang, K. N. Houk, Y. Tang, *J. Am. Chem. Soc.* **2019**, jacs.8b12010.
[59] A. Glöckle, T. A. M. Gulder, *Angew. Chem. Int. Ed.* **2018**, 2754–2756.
[60] H. J. Kim, M. W. Ruszczycky, S. H. Choi, Y. N. Liu, H. Liu, *Nature* **2011**, *473*, 109–112.
[61] N. Chen, F. Zhang, R. Wu, B. A. Hess, *ACS Catal.* **2018**, *8*, 2353–2358.
[62] Y. Zheng, W. Thiel, *J. Org. Chem.* **2017**, *82*, 13563–13571.
[63] Z. Yang, S. Yang, P. Yu, Y. Li, C. Doubleday, J. Park, A. Patel, B. Jeon, W. K. Russell, H. Liu, et al., *Proc. Natl. Acad. Sci. USA* **2018**, *115*, E848–E855.

[64] C. D. Fage, E. A. Isiorho, Y. Liu, D. T. Wagner, H. Liu, A. T. Keatinge-Clay, *Nat. Chem. Biol.* **2015**, *11*, 256–258.

[65] B. A. Hess, L. Smentek, *Org. Biomol. Chem.* **2012**, *10*, 7503–7509.

[66] E. G. Gordeev, V. P. Ananikov, *PLoS One* **2015**, *10*, 1–14.

[67] A. Patel, Z. Chen, Z. Yang, O. Gutiérrez, H. Liu, K. N. Houk, D. A. Singleton, *J. Am. Chem. Soc.* **2016**, *138*, 3631–3634.

[68] M. G. Medvedev, A. A. Zeifman, F. N. Novikov, I. S. Bushmarinov, O. V. Stroganov, I. Y. Titov, G. G. Chilov, I. V. Svitanko, *J. Am. Chem. Soc.* **2017**, *139*, 3942–3945.

[69] B. Jeon, M. W. Ruszczycky, W. K. Russell, G.-M. Lin, N. Kim, S. Choi, S.-A. Wang, Y. Liu, J. W. Patrick, D. H. Russell, et al., *Proc. Natl. Acad. Sci. USA* **2017**, *114*, 10408–10413.

[70] M. Ohashi, F. Liu, Y. Hai, M. Chen, M. Tang, Z. Yang, M. Sato, K. Watanabe, K. N. Houk, Y. Tang, *Nature* **2017**, *549*, 502–506.

[71] Z. Chang, T. Ansbacher, L. Zhang, Y. Yang, T.-P. Ko, G. Zhang, W. Liu, J.-W. Huang, L. Dai, R.-T. Guo, et al., *Org. Biomol. Chem.* **2019**, *7*, DOI 10.1039/C8OB02758G.

[72] Z. Tian, P. Sun, Y. Yan, Z. Wu, Q. Zheng, S. Zhou, H. Zhang, F. Yu, X. Jia, D. Chen, et al., *Nat. Chem. Biol.* **2015**, *11*, 259–265.

[73] M. J. Byrne, N. R. Lees, L. C. Han, M. W. van der Kamp, A. J. Mulholland, J. E. M. Stach, C. L. Willis, P. R. Race, *J. Am. Chem. Soc.* **2016**, *138*, 6095–6098.

[74] Q. Zheng, Y. Guo, L. Yang, Z. Zhao, Z. Wu, H. Zhang, J. Liu, X. Cheng, J. Wu, H. Yang, et al., *Cell Chem. Biol.* **2016**, *23*, 352–360.

[75] K. J. Hetrick, M. C. Walker, W. A. van der Donk, *ACS Cent. Sci.* **2018**, *4*, 458–467.

[76] D. P. Cogan, G. A. Hudson, Z. Zhang, T. V. Pogorelov, W. A. van der Donk, D. A. Mitchell, S. K. Nair, *Proc. Natl. Acad. Sci. USA* **2017**, *114*, 12928–12933.

[77] G. A. Hudson, Z. Zhang, J. I. Tietz, D. A. Mitchell, W. A. van der Donk, *J. Am. Chem. Soc.* **2015**, *137*, 16012–16015.

[78] W. J. Wever, J. W. Bogart, A. A. Bowers, *J. Am. Chem. Soc.* **2016**, *138*, 13461–13464.

[79] Z. Zhang, G. A. Hudson, N. Mahanta, J. I. Tietz, W. A. van der Donk, D. A. Mitchell, *J. Am. Chem. Soc.* **2016**, *138*, 15511–15514.

[80] S. R. Fleming, T. E. Bartges, A. A. Vinogradov, C. L. Kirkpatrick, Y. Goto, H. Suga, L. M. Hicks, A. A. Bowers, *J. Am. Chem. Soc.* **2019**, jacs.8b11521.

[81] P. Liu, E. N. Jacobsen, *J. Am. Chem. Soc.* **2001**, *123*, 10772–10773.

[82] B. Illarionov, W. Eisenreich, A. Bacher, *Proc. Natl. Acad. Sci. USA* **2001**, *98*, 7224–7229.

[83] B. Illarionov, I. Haase, A. Bacher, M. Fischer, N. Schramek, *J. Biol. Chem.* **2003**, *278*, 47700–47706.

[84] M. Breugst, A. Eschenmoser, K. N. Houk, *J. Am. Chem. Soc.* **2013**, *135*, 6658–6668.

[85] R. R. Kim, B. Illarionov, M. Joshi, M. Cushman, C. Y. Lee, W. Eisenreich, M. Fischer, A. Bacher, *J. Am. Chem. Soc.* **2010**, *132*, 2983–2990.

[86] G. W. E. Plaut, R. Beach, T. Aogaichi, *Biochemistry* **1970**, *9*, 771–785.

[87] A. Ramsperger, M. Augustin, A. K. Schott, S. Gerhardt, T. Krojer, W. Eisenreich, B. Illarionov, M. Cushman, A. Bacher, R. Huber, et al., *J. Biol. Chem.* **2006**, *281*, 1224–1232.

[88] T. Ose, K. Watanabe, T. Mie, M. Honma, H. Watanabe, M. Yao, H. Oikawa, I. Tanaka, *Nature* **2003**, *422*, 185–9.

[89] K. Watanabe, T. Mie, A. Ichihara, H. Oikawa, M. Honma, *J. Biol. Chem.* **2000**, *275*, 38393–38401.

[90] J. M. Serafimov, T. Westfeld, B. H. Meier, D. Hilvert, *J. Am. Chem. Soc.* **2007**, *129*, 9580–9581.

[91] J. M. Serafimov, D. Gillingham, S. Kuster, D. Hilvert, *J. Am. Chem. Soc.* **2008**, *130*, 7798–7799.

[92] C. R. W. Guimarães, M. Udier-Blagović, W. L. Jorgensen, *J. Am. Chem. Soc.* **2005**, *127*, 3577–3588.

[93] L. R. Domingo, J. A. Sáez, *Org. Biomol. Chem.* **2009**, *7*, 3576–3583.

[94] D. Hilvert, *Annu. Rev. Biochem.* **2000**, *69*, 751–793.

[95] J. Xu, Q. Deng, J. Chen, K. N. Houk, J. Bartek, D. Hilvert, I. A. Wilson, *Science* **1999**, *286*, 2345–2348.

[96] H. Kries, R. Blomberg, D. Hilvert, *Curr. Opin. Chem. Biol.* **2013**, *17*, 221–8.

[97] J. B. Siegel, A. Zanghellini, H. M. Lovick, G. Kiss, A. R. Lambert, J. L. St Clair, J. L. Gallaher, D. Hilvert, M. H. Gelb, B. L. Stoddard, et al., *Science* **2010**, *329*, 309–13.

[98] N. Preiswerk, T. Beck, J. D. Schulz, P. Milovnik, C. Mayer, J. B. Siegel, D. Baker, D. Hilvert, *Proc. Natl. Acad. Sci. USA* **2014**, 2–7.

[99] C. B. Eiben, J. B. Siegel, J. B. Bale, S. Cooper, F. Khatib, B. W. Shen, F. Players, B. L. Stoddard, Z. Popovic, D. Baker, *Nat. Biotechnol.* **2012**, *30*, 190–2.

[100] T. Sajed, A. Marcu, M. Ramirez, A. Pon, A. C. Guo, C. Knox, M. Wilson, J. R. Grant, Y. Djoumbou, D. S. Wishart, *Nucleic Acids Res.* **2016**, *44*, D495–D501.

[101] L. B. Davin, H. Bin Wang, A. L. Crowell, D. L. Bedgar, D. M. Martin, S. Sarkanen, N. G. Lewis, *Science* **1997**, *275*, 362–366.

[102] P. Yates, P. Eaton, *J. Am. Chem. Soc.* **1960**, *82*, 4436–4437.

[103] D. Hilvert, *Acc. Chem. Res.* **1993**, *26*, 552–558.

[104] A. Warshel, P. K. Sharma, M. Kato, Y. Xiang, H. Liu, M. H. M. Olsson, *Chem. Rev.* **2006**, *106*, 3210–35.

[105] T. Wang, T. R. Hoye, *Nat. Chem.* **2015**, *7*, 641–5.

[106] E. M. Stocking, R. M. Williams, *Angew. Chem. Int. Ed.* **2003**, *42*, 3078–3115.